

Matrix and donor/acceptor dependence of polymer dispersed pyrromethene dye photoconductivity

WADE N. SISK[†], KWANG-SUN KANG[†], M. YASIN AKHTAR RAJA[†] and FARAMARZ FARAH[†]

Transient photocurrent measurements were performed on pyrromethene dyes dispersed in polymer matrices to investigate the feasibility of these materials as the basis for novel optoelectronic devices. The photocarrier generation efficiency (PGE) was measured as a function of several parameters: polymer dielectric constant, donor/acceptor addition, temperature and light intensity. The PGE was found to increase with increasing polymer dielectric constant. Donor and acceptor dopants were found to enhance the photoconductivity of PM-567/polymer thin films. Triphenylamine was found to be the most effective dopant to enhance the PGE.

1. Introduction

Polymer optical materials doped with organic dyes and other light-sensitive materials are becoming very attractive for optoelectronic applications. A major drive comes from the new applications and promising technology for processing and manufacturing. Besides the low-cost advantage, polymer-based optoelectronic fabrication involves direct radiation-induced patterning of devices and waveguides without any additional photoresist layers or wet chemical etching [1]. There is also continuing interest in light-sensitive organic materials from their present use in xerography, photoresists, electrophotography and solar energy cells [2]. The various physical mechanisms include photoconductivity, non-linear phenomena and fluorescence. Photoconductivity, the production of an electrical current on the absorption of electromagnetic radiation, is the principle governing several applications. Thus, there is a continual need for new or more efficient photoconductors for the next generation of current and emerging optoelectronic applications. One of the novel optoelectronic applications is

the development of various optical modulators based on organic photoconductors such as optical amplitude modulators and switches. Present optical switches based on nonlinear optical fibres have the disadvantage of requiring high-power pulse lasers and a long interaction length of fibre to enhance their nonlinear effect [3–8]. It is likely that pyrromethene dyes, which possess high absorption cross-sections and high solubilities, could be used in the fabrication of field-dependent photoconductive optical switches.

Pyrromethene dyes are also currently used in solid-state dye lasers because of their high fluorescence quantum yield, low triplet-triplet absorption loss over the fluorescence spectral region, and high photostability [9, 10]. There is a continuing drive to produce solid-state dye lasers that not only bear significant quantum yields, but also have a high laser damage threshold. The relation between fluorescence yield and carrier generation for phthalocyanine compounds has been demonstrated by Popovic [11]; a higher fluorescence yield correlates with lower free carrier yield. The rational design of high efficiency solid-state dye lasers based on pyrromethene dyes may be improved by understanding the processes that compete with lasing, one of which is free carrier production.

Recently the photocarrier generation efficiency of pyrromethene dye/polymethylmethacrylate (PMMA) thin films have been investigated with regard to composition, temperature, excitation fluence and triphenylamine doping [12]. From the study it was concluded that the photocarrier generation efficiency had a maximum

Received 16 October 1995.

Authors' addresses: The authors are with the Optoelectronics and Quantum-Optics Group, University of North Carolina at Charlotte, 9201 University City Blvd., Charlotte, NC 28223, U.S.A. WNS and K-SK belong to the Chemistry Department Tel: +1 (704) 547 4433; Fax: +1 (704) 547 3151; e-mail: wsisk@unccvm.uncc.edu/kkang@unccvx.uncc.edu. MYAR and FF belong to the Physics Department-Tel: +1 (704) 547 2818/2826; Fax: +1 (704) 547 3160; e-mail: ffarahi@uncc.edu/raja@uncc.edu.

for a certain intermediate dye concentration and increased significantly on doping with triphenylamine, an electron donor. Photoconductivity in these organic materials originates from the production of electron-hole states (exciton states) via photoexcitation. These excitons may dissociate to form free carriers, or recombine to fluoresce, or relax by some non-radiative channel. The exciton dissociation process can be investigated by monitoring the resulting photocurrent under an external applied electric field.

Saito *et al.* [13] have measured the photocarrier generation efficiency of phthalocyanine-doped polymers under a strong external field ($\approx 10^5 \text{ V cm}^{-1}$) for several polymers differing in dielectric constant. Their results show that the photocarrier generation is strongly dependent on the polymer dielectric constant. This was attributed to the polymer's dielectric constant influencing the dissociation probability of the exciton pair. This can be understood by recognizing the fact that exciton radius increases with increasing dielectric constant due to the screening effect.

In this investigation the photocurrent of pyrromethene-dispersed polymers has been measured for a variety of polymers differing in dielectric constant. Several donor/acceptor additives, and their influence on photocarrier generation have been studied. In order to characterize this promising optoelectronic material, the photocarrier generation yield was also investigated as a function of temperature and photon fluence in order to obtain information on activation energies, trap distribution and photodegradation for the various compositions. The experimental details are given in section 2, and results are discussed in section 3. Finally, in section 4 the main results are summarized along with concluding remarks.

2. Experiment

2.1. Sample preparation

Various chemicals, dyes and dopants used in the studies are listed in table 1. In a typical case a small amount

$\approx 15 \text{ mg}$ of pyrromethene (PM-567) was added to 80 mg of polymer (Lexan-145, PMMA, PVB or PSR) and dissolved in 1.5 ml tetrachloroethane (TCE) for studies which compare different polymers. The sample preparation for donor/acceptor variation was performed by adding 71 mg of the selected additive (donors: TPA, TMPDA; and acceptors: DNB, TCNQ, DMBQ) to 1.14 g of stock solution {PM-567 (62 mg), PMMA (712 mg) and TCE (6 ml)}, such that the final composition was 1.054 g TCE, 78.9 mg PMMA, 71 mg additive (dopant), and 6.87 mg PM-567. In order to study the effect of donor/acceptor concentration on photoconductivity, a precise amount of PM-567/PMMA/TCE solution was taken and various amounts of dimethylbenzoquinone (DMBQ) were added by weight. These solutions were then spin-coated onto glass substrates with pre-deposited silicon oxide/indium-tin-oxide (ITO) films. A film thickness of $\approx 2 \mu\text{m}$ was achieved for the samples with polymer variation and $\approx 0.8 \mu\text{m}$ for the samples with dopant variation. Finally, at the top, aluminium electrodes were vacuum-deposited in 10^{-6} Torr vacuum conditions. The ITO film at the bottom layer serves as a transparent electrode.

2.2. Measurements

These samples were subjected to different applied voltages (0-120V) at a constant laser fluence ($\approx 1.05 \text{ mJ pulse}^{-1}$, 5mm diameter) to study the electric field dependence; for a fixed applied voltage ($\approx 40 \text{ V}$) the laser power dependence was studied with a variety of pulse energies in the range 0.60–2.48 mJ pulse^{-1} . The photodegradation as a function of number of shots was investigated by keeping the applied voltage in the range 20–80 V and laser pulse energy 2.48 mJ. The activation energies were obtained by varying the temperature from 25 to 82°C under the experimental conditions of applied voltages ranging from 2 to 80V and a laser energy of $1.05 \text{ mJ pulse}^{-1}$.

Figure 1 shows the apparatus used to measure the

Table 1. Chemical index for compounds used in this study (compounds were utilized without further purification)

Name	Acronym	Purity	Source
1,3,5,7,8-pentamethyl-2,6-diethylpyrromethene-difluoroborate complex	PM-567	$\approx 100\%$	Exciton Co.
polymethyl methacrylate	PMMA		Aldrich Chemical Co.
polyvinylbutyral	PVB		Aldrich Chemical Co.
polysulfone resin	PSR		Aldrich Chemical Co.
polycarbonate	Lexan-145		General Electric Co.
triphenylamine	TPA	98%	Aldrich Chemical Co.
N,N,N',N'-tetramethyl-p-phenylenediamine	TMPDA	98%	Acros Co.
m-dinitrobenzene	DNB	—	Matheson Coleman & Bell Co.
2,6-dimethyl benzoquinone	DMBQ	99%	Aldrich Chemical Co.
7,7,8,8-tetracyanoquino dimethane	TCNQ	98%	Aldrich Chemical Co.
1,1,2,2-tetrachloroethane	TCE	98%	Aldrich Chemical Co.

relative photocarrier generation efficiency. The samples were subjected to a 2ms long applied voltage square pulse generated by a signal generator (Stanford Research Systems DG535) and high-speed power amplifier (NF Electronics Instrument 4005). Near the middle of the voltage pulse the samples were excited by the second harmonic of Nd : YAG laser (532 nm, 5 ns, 3 Hz). The resulting photocurrent was detected across a 50 Ω resistor using a digital oscilloscope. The averaged signal (5–10 shots) was then time-integrated by a computer (sample signal). Background data was obtained by keeping all of the experimental conditions the same and blocking the laser light. The background was subtracted from the signal to obtain the correct photoresponse. The relative photocarrier generation efficiency (PGE) was determined as the ratio of the photoresponse divided by the absorbance at 532nm. The absorbance of the various samples was obtained using a UV-visible spectrometer (Shimadzu-2100).

In studying the temperature effect the absorbance was measured at a particular temperature, and this reference was used to correct the photoresponse at that temperature. Such normalization was necessary because the activation energy studies which measured photoresponse as a function of temperature were designed to determine the energy barrier starting from the excited state (S_1). The temperature was raised to increase the fraction of excited state molecules with enough energy to surpass the barrier for free carrier production from S_1 . Increasing the temperature was not intended to increase the number of excited state molecules, but invariably this does occur, owing to a temperature shift of the ground state Boltzmann distribution. This information is contained in the temperature dependence of the absorption coefficient. Thus, the excited-state temperature-dependent population differences may be accounted for by dividing

the photoresponse with the absorption coefficient at the given temperature. This will set the relative S_1 populations to be equal for different temperatures, such that the temperature variation affects the population distribution within the S_1 manifold and not the actual number of S_1 states. Unfortunately many researchers have neglected this correction, although it may be quite significant for certain molecules over a large temperature range.

3. Results and discussion

The photocarrier generation efficiency (PGE) and mechanism have been investigated in a variety of conditions and the results are given below.

3.1. Photocarrier generation efficiency field dependence

3.1.1. PGE field dependence and polymer variation. Figure 2 shows the dependence of the relative photocarrier generation efficiency (PGE) on the field strength for different polymers. The dielectric constants of the polymers are 4, 3.1, 3.1 and 2.9 for PMMA, PVB, PSR and Lexan, respectively. This trend is similar to the results of Saito *et al.* [13] for phthalocyanines; the PGE of pyrromethene dyes is also directly related to the dielectric constant of each polymer. Higher dielectric constant polymers provide a higher PGE. However, polyvinylbutyral (PVB) which has a dielectric constant of 3.1 displays an anomaly. This is attributed to the photochemical behaviour discussed below. The observations suggest that a high-polarity medium leads to greater free carrier production by reducing the exciton's lifetime, due to local field effects.

3.1.1. PGE field dependence and dopant variation. The redox potentials of dopants utilized in this study are listed in table 2 [14]. The rate of electron transfer can be

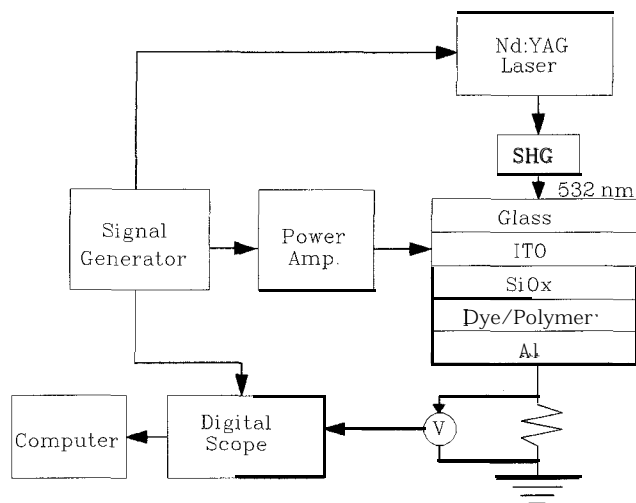


Figure 1. Schematic of transient photocurrent apparatus.

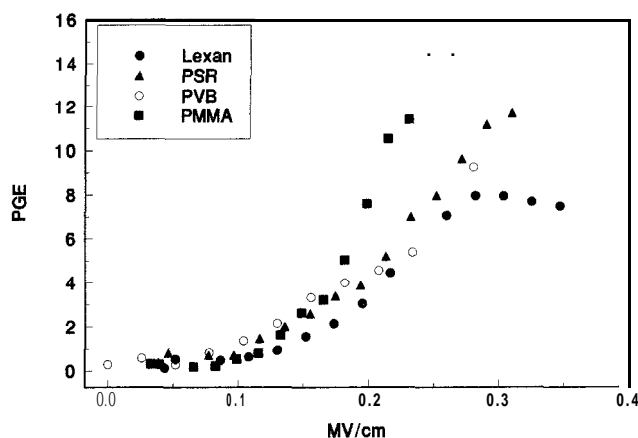


Figure 2. Field dependence of photoresponse normalized to absorption cross-section. Spin-coated thin films made from 15 mg PM-567 and 80 mg of polymer dissolved in 13 ml of TCE.

Table 2. Redox potentials obtained from reference 6. The listed half-wave potentials are written as reductions in CH₃CN solvent and SCE Ref Electrode. The reduction reaction corresponds to: A + e → A for electron acceptors and D⁺ + e → D for electron donors

Donor/ acceptor	Compound name	Half-wave potential
D	(TPA) triphenylamine	0.98
D	(TMPDA) N,N,N',N'-tetramethyl-p-phenylenediamine	0.46
A	(TCNQ) 7,7,8,8-tetracyanoquinodimethane	0.19
A	(DMBQ) 2,6-dimethyl-1,4-benzoquinone	-0.67
A	(DNB) 1,4-dinitrobenzene	-0.70

obtained using the Marcus relation, as suggested by Umeda *et al.* [15].

$$k_s = k_0 \exp \left[-\frac{(\lambda - \Delta E)^2}{4\lambda K_B T} \right] \quad (1)$$

$$\Phi = \Phi_{(CT \rightarrow e+h)} \frac{k_s}{k_s + k_L + K_{nr}}, \quad (2)$$

where k_s is the rate of electron transfer = CT, the production rate constant; k_0 is the pre-exponential factor; λ is the total reorganization energy (bond distance and bond angle change energies); ΔE is the energy gap (oxidation potential or reduction potential differences); K_B is the Boltzmann constant; Φ is the photocarrier generation efficiency; $\Phi_{(CT \rightarrow e+h)}$ is the probability of CT dissociation into free carriers; k_{nr} is the non-radiative decay constant; and k_L is the radiative decay constant.

The results of dopant addition are shown in figure 3. The behaviour in order of descending PGE is: TPA > DMBQ > DNB > TMPDA > TCNQ > no dopant. The interaction between the electron donor dopants (TMPDA and TPA) and an electron acceptor (PM-

567) may be described by a photoassisted charge transfer process: PM-567* + D ⇌ PM-567*⁻ + D⁺. The enhancement of photoconductivity for the acceptor dopants may be due to PM-567 behaving as an electron donor, since PM-567 is indeed a complex with localized charges. Previous studies with metal phthalocyanines and electron donors have shown an increase with acceptor addition and a decrease in photoconductivity with donor addition [16, 17]. In marked contrast, donor and acceptor additions to PM-567 have both led to an increase in photocarrier production. To be stoichiometrically correct, equal mole fractions (not equal weight fractions) should be compared. This still will not affect the general trend, since TPA has the highest molar mass.

Since there is no definite correlation between the PGE trend and ΔE (the energy gap), we may therefore conclude that ΔE alone is insufficient to explain the dopant-dependent trends in PGE. The total reorganization energy λ and other non-radiative quenching of the excited PM-567 must play a major role in determining the photocarrier generation yield. In amine molecules the neutral molecule is tetrahedral and its radical cation is planar. This may explain why TPA is a better donor than TMPDA, even though the oxidation potentials would suggest otherwise. It is possibly due to the large reorganization energy associated with the non-planar to planar geometry change that occurs upon electron transfer. In findings similar to this work, Fox *et al.* [18] recently concluded that the photocurrent production efficiency of indium tin oxide sandwich cells composed of metal octakis (β -decoxyethyl) porphyrins does not correlate directly with the solution phase oxidation potentials of the porphyrin series.

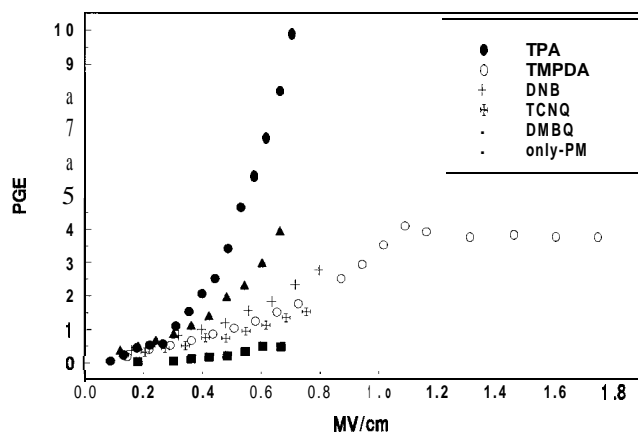


Figure 3. Photocarrier generation efficiency dopant variation. Spin-coated thin films made from 62 mg PM-567, and 712 mg of polymer dissolved in 13ml of TCE.

3.3.3. PGE field dependence variation with DMBQ concentration. Figure 4 shows the photocarrier generation efficiency as a function of DMBQ concentration. As can be seen, small additions of DMBQ were accompanied by an increase in photocurrent. This trend continues until a maximum photocurrent is obtained, after which continued additions of DMBQ resulted in a photocurrent decrease. Similar observations were made for

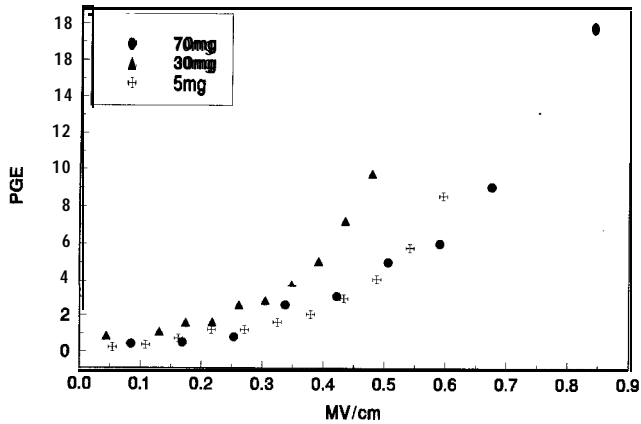


Figure 4. Photocarrier generation efficiency DMBO concentration dependence.

tetraphenylporphyrin dyes (p-type) doped with TCNQ [16]. We postulate that too much DMBO causes steric hindrance precluding favourable intermolecular interactions between pyrromethene molecules.

3.2. Light intensity dependent photoresponse

The effects of optical intensity were also investigated for a variety of conditions; the results are summarized below.

3.2.1. Polymer variation and light intensity dependence. The photoresponse of different polymers as a function of light intensity is illustrated in figure 5. The relation used to determine the intensity dependence is

$$R = KI^\alpha, \quad (3)$$

where R , K and I are the photoresponse, proportionality

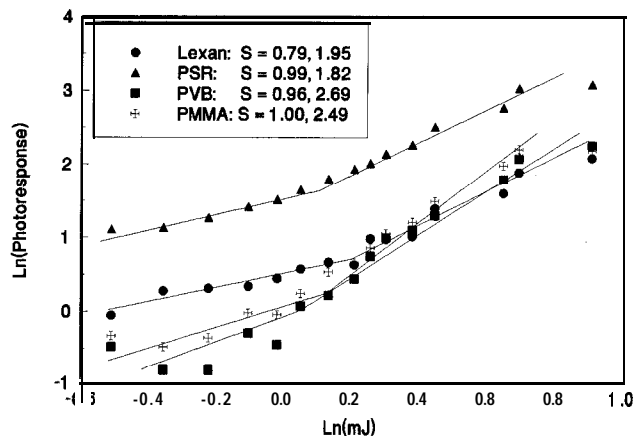


Figure 5. Natural logarithm plots of light intensity dependence of photocarrier generation efficiency with polymer variation. Laser pulse parameters are: 532nm wavelength, 4-6ns pulse width, 3 Hz repetition rate, 0.2-48 mJ pulse energy and a beam diameter of 0.5 cm.

constant and light intensity, respectively. The value of α is empirically determined as the slope via a linear least-squares fit. The variation of α from 0.5 to 1.0 is indicative of an exponential to uniform trap distribution [19, 20]. Polymers display PGE light intensity dependence behaviour at low and intense light levels, with $\alpha < 1$ and $\alpha > 1$, respectively. This interpretation of α as a trap description is quantitatively valid only if the experiments are conducted in the ohmic region, i.e. low fields where the photocurrent (photoresponse) varies linearly with the applied voltage. The low signal-to-noise ratio at low fields for PM-567 precluded operating in this region, the linear region of figures 2 and 3. Thus, light intensity variation experiments were conducted in the space-charge limited region, i.e. the field strengths for which the PGE varied nonlinearly. Nevertheless, the motivation for these experiments was to determine large changes in α indicative of a major change in the trap energy distribution. The region where $\alpha > 1$ is a manifestation of two classes of recombinant centres (i.e. different carrier capture cross-sections). The supra-linearity ($\alpha > 1$) comes about from the transition of a certain class of trap states to recombination centres, and is well documented for inorganic compounds such as CdSe and CdS [19, 20]. This begins at the same fluence point ($\approx 5.6 \text{ mJ cm}^{-2} \text{ pulse}^{-1}$) for each polymer, so the polymer has little effect on the light intensity transition point from sublinear ($\alpha < 1$) to supralinear dependence. Conservatively, it has little effect on the trap distribution. Thus for these polymer-varied samples, as the fluence becomes greater than $5.6 \text{ mJ cm}^{-2} \text{ pulse}^{-1}$, a major trap energy distribution change occurs due to the conversion of trap states to recombination centres.

3.2.2. Dopant variation and light intensity dependence. The dependence of photoresponse on light intensity for different dopants is shown in figure 6. All dopants except TPA exhibit a sublinear-supralinear transition within the fluence range studied. Triphenylamine doped samples display a sublinear ($\alpha \approx 0.6$) dependence in this range. This may be attributed to TPA addition causing a change in the trap distribution, since α drops from ~ 1.0 to 0.6. A similar decrease in α has been reported for trivalent metal phthalocyanines doped with electron acceptors O_2 and NO_2 [17]. The value of α is very much dependent on the polymer and/or dopant.

3.3. Photodegradation

These materials are potential candidates for optoelectronic devices, where the efficiency and reliability are the key issues. For these materials to be considered for optoelectronic devices, the photodegradation

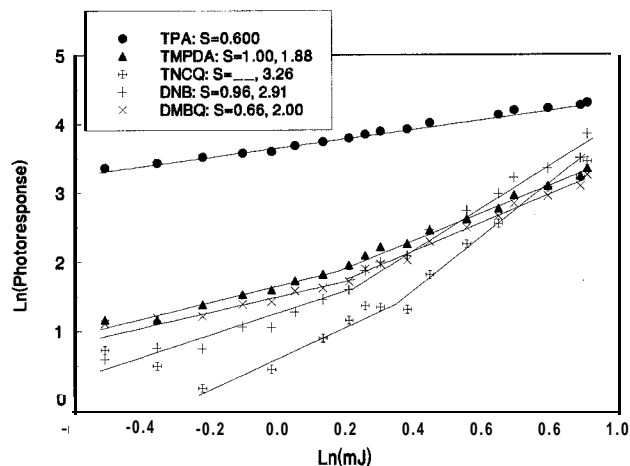


Figure 6. Natural logarithm plot of light intensity dependence of photocarrier generation efficiency with dopant variation. Laser pulse parameters are 532nm wavelength, 4–6 ns pulse width, 3 Hz repetition rate, 0–2.48 mJ pulse energy, and a beam diameter of 0.5 cm.

characteristics need to be studied. The rate of laser-induced degradation was determined by monitoring the photoreponse as a function of laser shots with a fluence of $12.6 \text{ mJ cm}^{-2} \text{ pulse}^{-1}$. For a 5 ns pulse this translates to a peak power of $2.5 \times 10^6 \text{ W cm}^{-2}$. The lifetimes (defined here as the time for 50% reduction of photoreponse) for

different polymer and dopant variations are tabulated in table 3.

For the polymer variation as shown in figure 7 (a–c), the photodegradation rate (inverse of lifetimes) increased with increasing field strength for PMMA and PSR, but decreased with increasing field strength for Lexan-145. Polyvinyl butyryl (PVB) displayed odd photodegradation behaviour; initially the photoreponse increased with the number of laser shots, reached a maximum and then decreased with subsequent laser shots, as shown in figure 7(d). In contrast with the laser intensity studies, the photodegradation measurements are strongly polymer-dependent. Previous studies on the photodegradation of dye-doped-polymers have determined this to be a photothermal process in which the dye serves as a ‘molecular heater’ [21]. Photodegradation proceeds by internal conversion of the electronic energy of the dye molecule to high vibrations of the ground state, followed by intramolecular vibrational redistribution, and transfer of the vibrational energy of the dye molecule to the phonon modes of the polymer matrix [21]. The efficiency with which the polymer transfers this energy may lead to radical formation. Subsequent reaction of these radicals leads to polymer-dependent photodecomposition. If this radical formation scheme is valid, a logical consequence is that the observed photodecay profiles should agree with the predicted photodegradation profile. The photodegradation curves could not be fit to an exponential expression

Table 3. Energy/pulse= 2.49 mJ, beam diameter = 0.5 cm

polymer	Polymer variation			Dopant variation																	
	thickness (μm)	field strength (MV cm^{-1})	half life (no. of shots)	dopant in PMMA	thickness (μm)	field strength (MV cm^{-1})	half life (no. of shots)														
Lexan	2.31	$\left\{ \begin{array}{l} 0.347 \\ 0.304 \\ 0.217 \\ 0.13 \end{array} \right.$	$\left\{ \begin{array}{l} 1480 \\ 1470 \\ 1150 \\ 910 \end{array} \right.$	TPA	1.129	$\left\{ \begin{array}{l} 0.62 \\ 0.531 \\ 0.443 \\ 0.354 \end{array} \right.$	$\left\{ \begin{array}{l} >4000 \\ >4000 \\ 2600 \\ 2330 \end{array} \right.$														
								PSR	$\left\{ \begin{array}{l} 0.116 \\ 0.078 \\ 0.039 \end{array} \right.$	$\left\{ \begin{array}{l} 320 \\ 720 \\ 1450 \end{array} \right.$	TMPDA	0.69	$\left\{ \begin{array}{l} 0.813 \\ 0.726 \\ 0.581 \\ 0.436 \end{array} \right.$	$\left\{ \begin{array}{l} 1030 \\ 560 \\ 480 \\ 650 \end{array} \right.$							
															PMMA	$\left\{ \begin{array}{l} 0.198 \\ 0.165 \\ 0.132 \end{array} \right.$	$\left\{ \begin{array}{l} 800 \\ \\ 1540 \end{array} \right.$	DNB	0.73	$\left\{ \begin{array}{l} 0.956 \\ 0.796 \\ 0.637 \\ 0.478 \end{array} \right.$	$\left\{ \begin{array}{l} 3300 \\ 2780 \\ 2580 \\ 1640 \end{array} \right.$
								DMBQ	0.83	$\left\{ \begin{array}{l} 0.604 \\ 0.483 \\ 0.362 \\ 0.242 \end{array} \right.$	$\left\{ \begin{array}{l} 1620 \\ 1210 \\ 1390 \\ 1300 \end{array} \right.$										

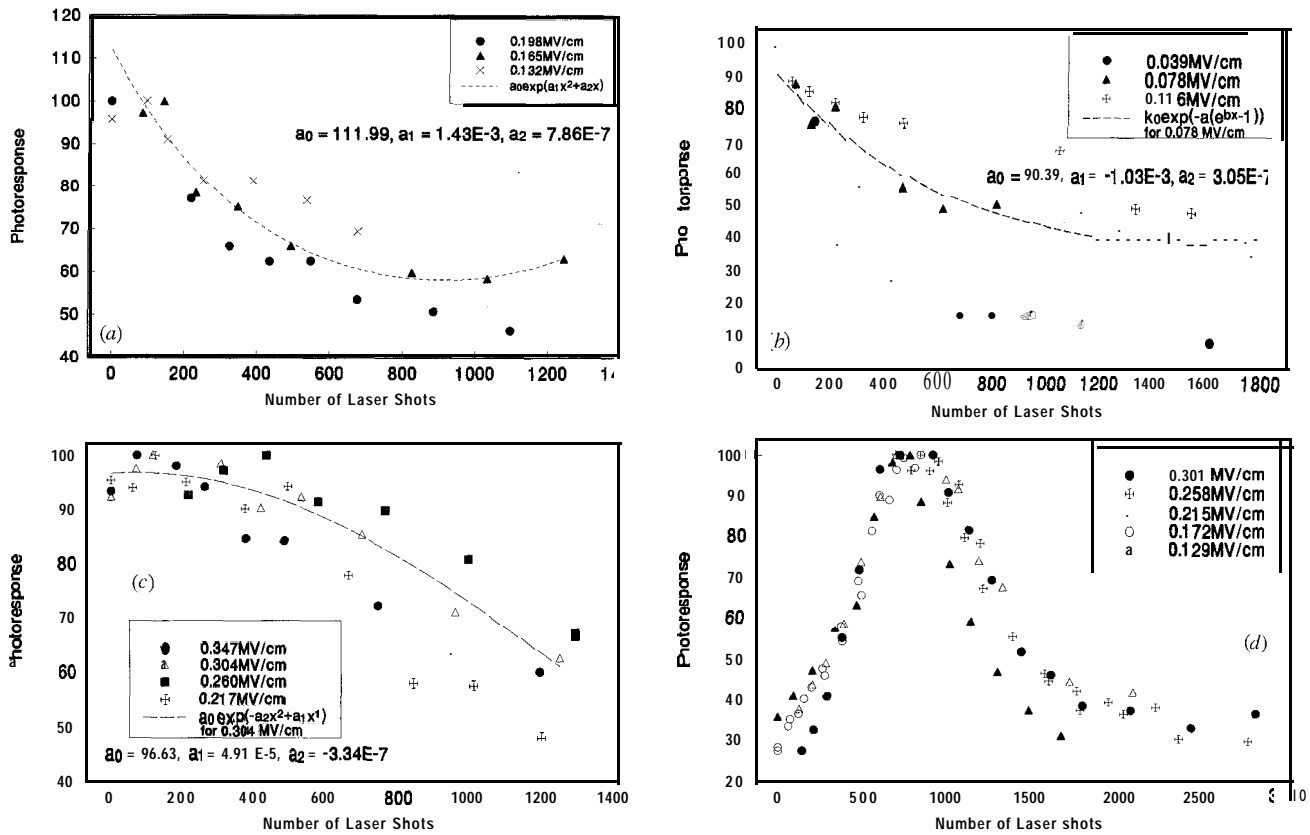


Figure 7. Laser-induced photodegradation at a pulse energy of 2.48 mJ: (a) PM-567/PMMA; (b) PM-567/PSR; (c) PM-567/Lexan-145; and (d) PM-567/PVB. The degradation is detected as a decrease in the photoresponse.

$k_0 \{ \exp[-a(e^{bx} - 1)] \}$ previously used to fit lasing output for Rhodamine 6G/PMMA films via a radical-induced decay model [22] (where k_0 is the initial photoresponse, and a and b are fitting parameters, and x is the number of shots). An empirical expression $a_0 \{ \exp[a_1 x' + a_2 x'^2] \}$ proved to be a better fitting function (where a_0 , a_1 , and a_2 are fitting parameters). The present studies differ from previous lasing [22] studies, not only in terms of the observable (lasing versus photoresponse), but also the concentration in the present photocurrent study is 10^3 – 10^5 times higher than that of the lasing study. Higher concentration leads to higher aggregate formation. It is postulated that these aggregates may facilitate radical formation, and hence increase the photodegradation rate. The inequivalence of fluorescence (lasing) decay and photoresponse decay may involve the creation of traps. For example, several hundred laser pulses could lead to traps which prevent the free carriers from migrating to the electrodes, thus leading to a reduction of photocurrent. If this were the dominant factor, the photodegradation rate should decrease with increasing field strength, as in the case of Lexan-145. However, the picture is more complicated than this because an increase in the field means an increase in the number of free carriers, and

a free carrier concentration-dependent process may lead to faster decomposition rates with increasing field strengths, as in the case of PMMA and PSR. More insight into the photoresponse decay could be obtained if the laser were to pulse under zero field conditions, and a strong collection field were applied immediately thereafter.

In the case of different dopants, generally as the external field strength increased, the photodegradation lifetimes increased slightly. Figures 8(a) and 8(b) illustrate this decay for TPA- and DMBQ-doped samples. However, for TCNQ the opposite was true: an increase in field strength led to a decrease in lifetime. The increase in lifetime for donor/acceptor doped samples with field strength may be reasoned as follows. The dissociation of the extrinsic CT state into free carriers competes with the energy transfer degradation channel. Increasing the field strength leads to greater dissociation of the CT complex, thus reducing the chances of recombination and photodegradative energy transfer. The TCNQ-doped samples had limited solubility of TCNQ, as evidenced by the TCNQ aggregates observed in the film; thus, few extrinsic CT complexes are formed. If this is the case, then the sample may behave similar to the undoped PMMA samples.

3.4. Temperature variation

The photoresponse was measured as a function of temperature for several polymer and dopant samples. An initial photoresponse decrease accompanied the temperature increase; however, further heating led to a photoresponse increase. This is shown in figure 9 for samples doped with TPA. This is yet another manifestation of the transition from one to two recombination centres. One class of traps are those undergoing the transition from trap to recombination centre, during which time the photoresponse is decreasing with rising temperature [19, 20]. Similar to previous work [12] for PM-567/PMMA, the activation energies for the totally transformed samples may be obtained from the logarithmic plots of photoresponse versus T^{-1} for temperatures above the critical point. The zero-field activation energy 0.14 eV for the TPA doped samples was obtained by extrapolating the activation energy with field strength (figure 10). This is higher than 0.11 eV for pure PM-567/PMMA films [12]. This result is peculiar, in that enhanced photoresponse is observed from dopant addition, thus a lower activation energy would be anticipated. However, caution must be

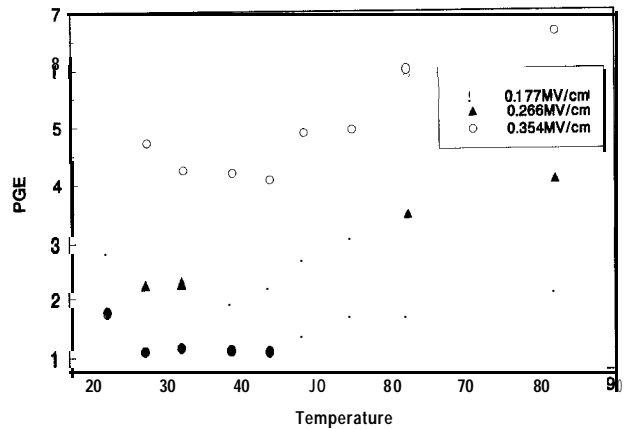


Figure 9. Temperature dependence of photocarrier generation efficiency for PM-567/TPA/PMMA.

exercised at utilizing these activation energies, since two temperature-dependent processes are occurring in this region: transformation of traps to recombination centres and an increase in the Boltzmann population above the activation barrier.

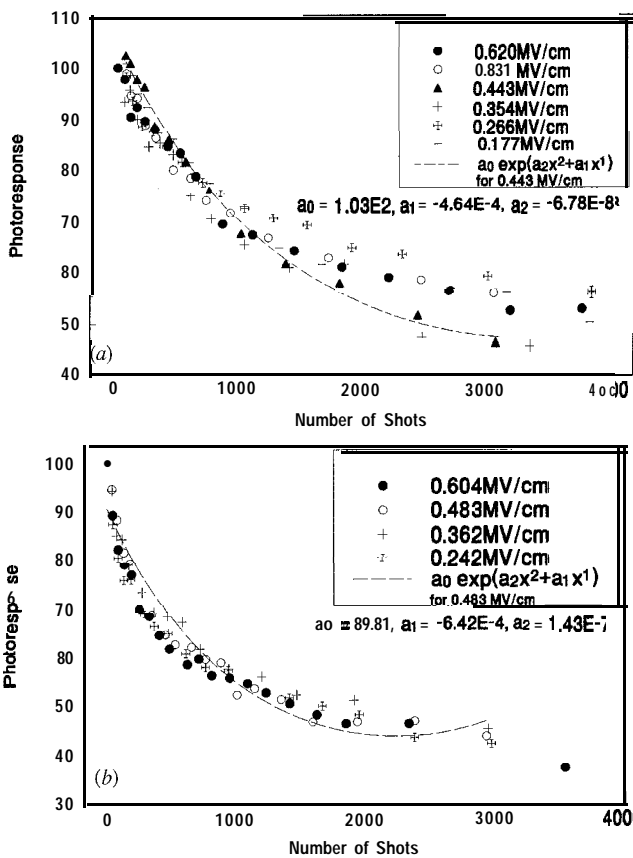


Figure 8. Photodegradation as shown by a decrease in the photoresponse at a pulse energy 2.48 mJ: (a) PM-567/TPA/PMMA; and (b) PM-567/DMBQ/PMMA.

4. Conclusion

The photocarrier generation efficiency was found to increase with increasing polymer dielectric constant. Both electron acceptor and donor addition enhanced the photocarrier generation efficiency of PM-567/polymer films. Triphenylamine was found to be the dopant most effective in enhancing the photocarrier generation efficiency. A change in the trap energy distribution was observed for increasing temperature and laser fluence, indicative of a trap to recombination centre transition. Dopant addition led to slower photodegradation rates. Based on the photoresponse yield and photodegradation rate, the composition suitable for optoelectronic devices should consist of PM-567 dye, triphenylamine

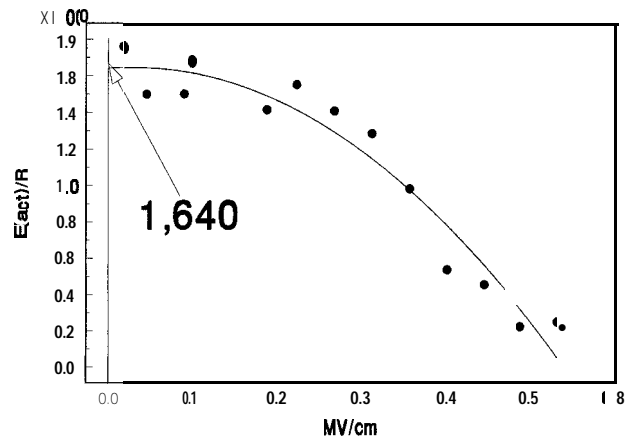


Figure 10. Activation energy of PM-567/TPA/PMMA films.

and polymethacrylate. We are currently fabricating the devices in order to characterize the material and its utility for optical switches based on this composition.

Acknowledgments

The authors would like to thank Mr John Hudak of Cameron Applied Research Center for his technical assistance.

References

- [1] HORNAK, L. A., 1992, *Polymers for Lightwave and Integrated Optics* (New York: Marcel Dekker).
- [2] GUILLET, J., 1985, *Polymer Photophysics and Photochemistry* (New York: Cambridge University Press).
- [3] DORAN, N. J., FORRESTER, D. S., and NAYAR, K., 1989, *Electron. Lett.*, *25*, 267.
- [4] BLOW, K. J., DORAN, N. J., and NAYAR, B. K., 1989, *Opt. Lett.*, *14*, 754.
- [5] BLOW, K. J., DORAN, N. J., NAYAR, B. K., and NELSON, B. P., 1990, *Opt. Lett.*, *15*, 248.
- [6] FARRIES, M. C., and PAYNE, D. N., 1989, *Appl. Phys. Lett.*, *55*, 25.
- [7] FIRBERG, S. R., WEINER, A. M., SILBERBERG, Y., and SMITH, P. W., 1988, *Opt. Lett.*, *13*, 904.
- [8] TRILLO, S., WANITZ, S., FINLAYSON, N., BANYAI, W. C., SEATON, C. T., STEGEMAN, G. I., and STOLEN, R. H., 1988, *Appl. Phys. Lett.*, *53*, 837.
- [9] TRUSSELL, C. W., 1994, The potential of solid state dye lasers. *Proc. Solid-state Dye Laser Technology Workshop*, Fort Belvoir, Virginia, U.S.A., August.
- [10] PAVLOPOULOS, T. G., BOYER, J. H., SHAH, K. T., and SOONG, M., 1990, *Appl. Optics*, *29*, 3885.
- [11] POPOVIC, Z. D., 1982, *J. Chem. Phys.*, *76*, 2714.
- [12] KANG, K., SISK, W. N., FARAH, F., and RAJA, M. Y. A., 1995, PhotocARRIER generation efficiency of pyrromethene-doped polymers. *Proc. Organic Thin Films for Photonic Applications*, Portland, Oregon, U.S.A., 9-14 September, pp. 109-112.
- [13] SAITO, T., KAWANISHI, T., and KAKUTA, A., 1991, *Japan J. Appl. Phys.*, *30*, L1182.
- [14] MEITES, L., 1977, *CRC Handbook Series in Organic Electrochemistry* (New York: CRC Press).
- [15] UMEDA, M., SHIMADA, T., ARUGA, T., NIIMI, T., and SASAKI, M., 1993, *J. Phys. Chem.*, *97*, 8531.
- [16] HARIMA, Y., YAMAMOTO, K., TAKEDA, K., and YAMASHITA, K., 1989, *Bull. Chem. Soc. Japan*, *62*, 1458.
- [17] PANKOW, J. W., ARBOUR, C., DODELET, J. P., COLLINS, G. E., and ARMSTRONG, N. R., 1993, *J. Phys. Chem.*, *97*, 8485.
- [18] FOX, M. A., PAN, H., JONES, JR., W., and MELAMED, D., 1995, *J. Phys. Chem.*, *99*, 11523.
- [19] ROSE, A., 1978, *Concepts in Photoconductivity and Allied Problems* (New York: Robert E. Krieger).
- [20] BUBE, R. H., 1992, *Photoelectronic Properties of Semiconductors* (New York: Cambridge University Press).
- [21] CHEN, S., LEE, I. Y., TOLBERT, W. A., XIAONING, W., and DLOTT, D. D., 1992, *J. Phys. Chem.*, *96*, 7178.
- [22] GROMOV, D. A., DYUMAEV, K. M., MANENKOV, A. A., MASLYUKOV, A. P., MATYUSHIN, G. A., NECHITAILO, V. S., and PROKHOROV, A. M., 1985, *J. Opt. Soc. Am.*, *B2*, 1028.